Controlled Molecular Conformation and Morphology in Poly(amidoamine) (PAMAM) and Poly(propyleneimine) (DAB) Dendrimers

Bertrand Donnio,[†] Joaquín Barberá,[‡] Raquel Giménez,[‡] Daniel Guillon,[†] Mercedes Marcos,[‡] and José Luis Serrano*[,‡]

Química Orgánica, U.E.I. Nuevos Materiales Orgánicos, Facultad de Ciencias, Instituto de Ciencia de Materiales de Aragón, Universidad de Zaragoza-CSIC, E-50009 Zaragoza, Spain, and Institut de Physique et Chimie des Matériaux de Strasbourg, UMR 7504, Groupe des Matériaux Organiques, 23, rue du Loess, F-67037 Strasbourg Cedex, France

Received May 21, 2001; Revised Manuscript Received September 27, 2001

ABSTRACT: The mesomorphic behavior of several new end-functionalized liquid-crystal-containing dendrimers is reported. These liquid-crystalline dendrimers are obtained by attaching promesogenic units to the termini of the preexisting first five generations of poly(amidoamine) (PAMAM) and poly(propyleneimine) (DAB) polymers by a condensation reaction; the promesogenic units are derived from salilcylaldimine bearing one, two, or three terminal aliphatic chains. All of the compounds were found to exhibit liquid-crystalline properties, as deduced by polarized-light optical microscopy (POM) observations, differential scanning calorimetry (DSC) measurements, and X-ray diffraction (XRD) studies. The nature of the liquid-crystalline behavior of the dendrimers is directly correlated with the number of terminal chains grafted on the peripheral anisotropic groups. Indeed, the presence of one chain per mesogenic unit favors their parallel arrangement; hence, smectic mesomorphism (SmA and SmC) is induced. Increasing the number of aliphatic chains (two and three) favors their radial disposition, leading to the formation of columnar structures (Col_H). The differences in the thermal behaviors observed for these systems are discussed in terms of generation number, dendritic core, and number of terminal alkoxy chains. Considering the amphipathic character of the dendrimers (in this case, the incompatibility between the different constitutive molecular segments), which leads to microphase segregation, and the conformation of the dendritic core, a general model for the description of the molecular organization within the different types of supramolecular arrangements (lamellar and columnar mesophases) is proposed.

Introduction

During the past 20 years, macromolecular chemists have witnessed the growth of a new, innovative, and interdisciplinary area of research dealing with the synthesis and study of highly branched polymers or cascade molecules also known as dendrimers.[1] What makes dendritic compounds original and remarkable with respect to other high-molecular-weight compounds is that they exhibit three-dimensional fractal structures and molecular dimensions on the nanoscopic scale and they have the possibility to carry a large number of functional groups. The combination of precise functionalities at the termini or in the cavities with large and defined macromolecular structures offers many opportunities in materials science and medicine as well as many fundamental aspects. For example, these compounds can be used for the construction of materials with new technological applications based on a wide spectrum of properties (chemical, physical, optical, multiredox, and catalytic) in host−guest chemistry (encapsulation of guests in the cavities of dendritic hosts) and in self-assembly, molecular recognition, and biomimetism for medical and pharmaceutical purposes.[1] Furthermore, these macromolecules are unique in that they lack entanglements, leading to good solubility in almost all organic solvents and, in principle, to a lower intrinsic viscosity.

Among this fascinating class of highly functional compounds, dendrimer-containing thermotropic liquid crystals (LC dendrimers) are of special interest because of the possibility of creating controlled multifunctional macromolecular objects that are able to self-assemble into large organized assemblies. Such macromolecules are attractive candidates in the field of material science and could represent an original concept for the realization of molecular electronic-based devices. They are also of academic interest because they combine two opposite tendencies: the structural anisometric units, which will preferentially favor anisotropic order (enthalpic gain), and the flexible dendritic architecture from which the branches tend to radiate isotropically, leading to a pseudospherical morphology (entropic gain). LC dendrimers can be regarded as block molecules, in analogy to block copolymers, in that the dendritic core and the functionalized terminal groups (mesogenic, promesogenic, or nonmesogenic) will tend to microphase separate because of their incompatible chemical natures.[2] The mesomorphic properties (phase type, transition temperatures, and thermodynamic stability) thus highly depend on the enthalpy/entropy balance (core conformation), the degree of chemical incompatibility, and the sizes of the different building blocks (and thus of the microsegregated domains), as well as the structure of the mesogenic unit itself and its location in the dendrimer. In general, the terminal units determine the nature of the mesomorphism of the entire compound, the dendritic architecture being used as the scaffold only.

* Author to whom correspondence should be addressed. Fax and phone: (+) 34 976 761209. E-mail: joseluis@posta.unizar.es.
[†] Institut de Physique et Chimie des Matériaux de Strasbourg.
[‡] Universidad de Zaragoza-CSIC.

10.1021/ma010881+ CCC: $22.00
Published on Web 12/18/2001

Chart 1

PAMAM[L_x]$_n$ or **DAB[L_x]$_n$** where: **L** = mesogenic unit

x = number of terminal chains per mesogenic unit

n = number of mesogenic units

PAMAM dendrimers:

DAB dendrimers:

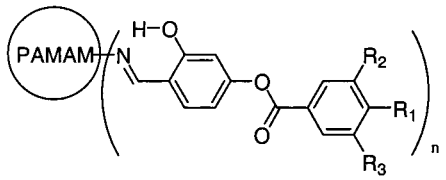

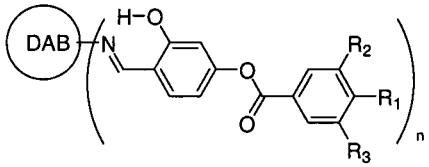

PAMAM[L_1]$_{4,8,16,32,64}$: $R_1 = OC_{10}H_{21}$, $R_2 = R_3 = H$

PAMAM[L_2]$_{4,8,16,32,64}$: $R_1 = R_2 = OC_{10}H_{21}$, $R_3 = H$

PAMAM[L_3]$_{16}$: $R_1 = R_2 = R_3 = OC_{10}H_{21}$

DAB[L_1]$_{4,8,16,32,64}$: $R_1 = OC_{10}H_{21}$, $R_2 = R_3 = H$

DAB[L_2]$_{4,8,16,32,64}$: $R_1 = R_2 = OC_{10}H_{21}$, $R_3 = H$

DAB[L_3]$_{16}$: $R_1 = R_2 = R_3 = OC_{10}H_{21}$

The field of LC dendrimers has now properly expanded, and when suitably designed, several structures[3−12] have been found to be compatible with the formation of liquid crystals. The structurally perfect dendrimers (considered here) exhibit a well-defined architecture, with a controlled number of branches (and thus a defined number of functional moieties) as a consequence of their layer-wise construction. These dendrimers are built outward from (or inward toward) a central core moiety by an iterative type of synthesis consisting of successive and controlled elementary steps. Such a sequential mode of construction thus leads to practically monodisperse systems. A perfect control of the number of terminal groups (which increases exponentially with generation number) is therefore achieved, and more accurate structural comparisons are then made possible.

The work reported in this article is part of a research program on the design of new mesomorphic materials. One aspect is to understand the structure−property relationships of end-functionalized LC dendrimers and to determine some structural criteria involved in their self-assembly and self-organization processes. Such understanding is of general interest in view of constructing tailored functional nanomaterials. In previous articles, some of us have reported the synthesis and characterization of new poly(amidoamine) (PAMAM)[6b,c] and poly(propyleneimine) (DAB)[7g] end-functionalized LC dendrimers. A significant number of new compounds have been synthesized for this study. The rigid anisotropic units, namely, salilcylaldimine derivatives bearing one or more terminal alkoxy chains, are attached terminally to the peripheral amino groups of several preexisting dendritic polymers of various generations. In this paper, we present a comparative study of the mesomorphic behavior between homologous series of PAMAM and DAB dendrimers carrying these promesogenic groups and, in particular, the influence of their substitution patterns on the mesomorphism observed, as well as two descriptive models showing the molecular organization within the smectic and columnar mesophases. The models should also permit the description of other supramolecular assemblies, such as cubic mesophases, generated by other LC dendrimers, allowing for the prediction of mesomorphic properties and more appropriate molecular design.

Results

The compounds discussed in this study are schematically represented in Chart 1. As often observed in liquid-crystalline polymers, the grafting of poorly mesogenic groups (or nonmesogenic anisotropic units) onto a polymeric chain often results in the improvement (or the induction) of the mesomorphic properties compared to those of the low-molar-weight monomers. In the present work, the same phenomenon of mesophase stabilization or induction occurs in that the coupling of promesogenic moieties to the dendritic PAMAM and DAB polymers yields new high-molar-weight liquid crystals. The salilcylaldimine units prepared for this work as model compounds (that contain a N-decyl group) are either poor liquid crystals or not mesomorphic at all: the one-chain compound shows a narrow range of SmC and N phases with a clearing temperature of 80 °C, whereas the two- and three-chain derivatives are obtained as amorphous solids or oils deprived from any mesomorphic behavior.

The general mesomorphism observed for these different families of dendrimers can be understood a priori by using simple structural arguments based on the chemical incompatibilities between the different constitutive parts and the two possible conformations that the molecules can adopt, i.e., *parallel* or *radial* (Figure 1). The existence of the mesophases results in large part from the formation of layer-block structures being driven by microphase separation between the incompatible constituting segments of the molecule (dendritic network, rigid aromatic parts, and aliphatic chains), which is, to some degree, reinforced by the anisotropic interactions between the rigid mesogenic units. The change in the number of terminal chains per end group (L_x, $x = 1, 2, 3$) also modifies the relationships between the hard part and the soft peripheral part (alkoxy chains) and thus the nature of the mesophase.

As will be seen from the results presented in the following diagrams and tables, all of the L_1-based compounds show a lamellar morphology (and a nematic

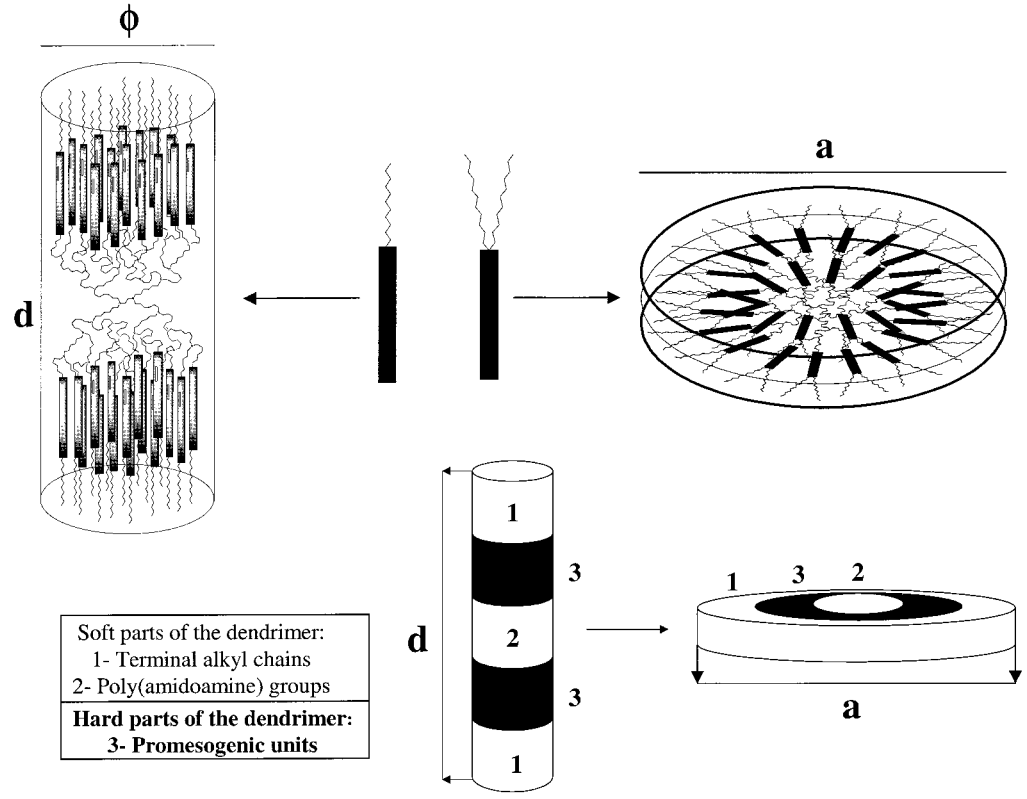

Figure 1. Schematic representation of the two main molecular conformations (parallel and radial) of end-functionalized liquid-crystalline dendrimers and their relationships with the number of grafted terminal alkoxy chains. The giant rods and disks are formed by the microsegregation of the different incompatible segments in an analogy with block copolymers.

phase for one compound only), whereas the L_2- and L_3-based systems show columnar mesophases, independently of the nature of the dendritic matrix. The formation of lamellar mesophases in the L_1-based systems is the result of the parallel disposition of the mesogenic groups on the two sides of the dendritic matrix: in this case, the dendrimer adopts the shape of a giant rod (Figure 1), with these groups then organizing into layers. However, the grafting of additional terminal chains at the periphery of the rigid anisotropic units prevents this parallel disposition of the promesogenic groups (L_2- and L_3-based systems), which are then forced to be radially arranged around the central moiety (Figure 1): the dendrimer can adopt the shape of a flat, tapered object, which will self-arrange into supramolecular disks or a disk shape. This leads to the formation of supramolecular columns by a self-assembly process; then, these columns further self-organize into columnar mesophases. A more specific and detailed description of the thermal behavior of all of the compounds is given hereafter.

Synthesis and Characterization

The new dendrimers were synthesized in the same manner as the previous ones[6b,6c,7g] by a condensation reaction between the appropriate salicylaldehyde derivative and the terminal amino groups of the corresponding generation of dendrimer (PAMAM or DAB). All of the compounds were isolated as air-stable solids and are soluble in solvents such as dichloromethane, chloroform, and THF but insoluble in ethanol.

The purity of these compounds was established using gel permeation chromatography (GPC) and elemental analysis, and results from ^{1}H and ^{13}C NMR and IR spectroscopy and FAB^+ mass spectrometry were in agreement with the expected structures. Evidence for the condensation reactions was provided by the lack of a signal at $\delta = 195$ ppm in the ^{13}C NMR spectra (which corresponds to the carbonyl of the aldehyde), along with the complete absence of NH_2 signals from the starting compound in the ^{1}H NMR and IR spectra. The molecular masses of the higher-molecular-weight dendrimers ($M \geq 5000$) could not be measured with FAB-MS technique. In contrast, the lower-molecular-weight dendrimers ($M < 5000$) exhibited FAB^+ spectra that contain peaks for $[M^+ - 3]$ and $[M^+ + Na]$ ions. GPC measurements (mobile phase, THF; calibration standard, polystyrene) confirmed the presence of practically monodisperse polymers in all cases. However, as is often the case with dendrimers, a deviation from the calculated molecular weight was found in the experimental data even for the low-molecular-weight compounds.

Mesomorphic Properties

The liquid-crystalline properties of these dendrimers were examined and characterized by polarized-light optical microscopy (POM) and differential scanning calorimetry (DSC) prior to X-ray diffraction (XRD). The previously described dendrimers, PAMAM$[L_1]_n$, PAMAM-$[L_2]_n$, and DAB $[L_1]_{4,8}$[6b,6c,7g] have been included in this work so that, first, suitable and significant comparisons could be performed and some structural relationships determined and, second, the validity of the models proposed for the molecular organization into the lamellar and columnar mesophases when applied to all of them could be tested. In addition, a dilatometry experiment was carried out on the monomer in order to refine the models of the molecular organization.

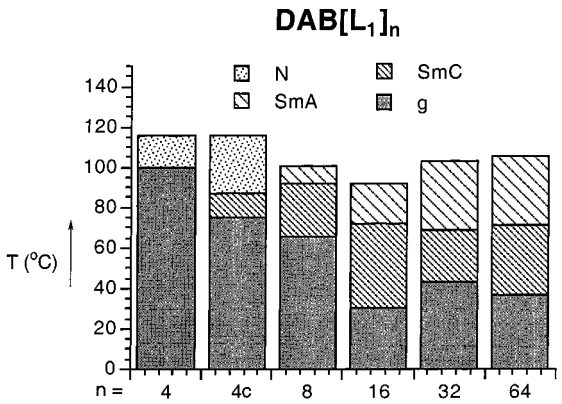

Figure 2. Phase behavior of DAB$[L_1]_n$. For compound DAB-$[L_1]_4$, the second heating (n= 4) and second cooling (n= 4c) are displayed.

DSC Measurements. These dendrimers behave as typical polymers , and in general, the DSC traces appear complicated in the first heating scan. However, in the second scan after an annealing process (15 min in the isotropic liquid), very simple thermograms are obtained. They are all qualitatively similar and consist of two or three endotherms, separating three or four different regions. In most cases, one can distinguish an anisotropic glass-to-mesophase transition at T_g, a mesophase-to-mesophase transition for some of them, and a mesophase-to-isotropic liquid transition at T_i. Subsequent heating−cooling cycles up to the isotropic liquid showed the same behavior, an indication of the good thermal stability of the compounds.

POM Observations. The liquid-crystalline behavior of these dendrimers was partially confirmed by the POM observation of the optical textures of the mesophases. Unfortunately, this technique was not totally conclusive in giving unequivocal information concerning the assignment of the mesophase. Nevertheless, some specific textures associated with those exhibited by smectic C and smectic A phases could be recognized in some cases, namely, both blurred and Schlieren textures for the former and a homeotropic texture observed when a mechanical shear was applied to the sample for the latter. In the following discussion, the mesophases will be referred as SmC and SmA phases, respectively, on the basis of the above observations, although some precautions must be taken as it is quite unlikely that liquid-crystalline dendrimers display smectic mesophases that are identical to those of purely calamitic systems. Instead, they probably self-organize into a more complex lamellar morphology, in an evident relationship with their unique molecular architecture. The columnar mesophase does not show any characteristic feature, although, in some cases, a broken fanlike texture can be identified. Taking these comments into account, the mesomorphic properties of the PAMAM and DAB dendrimers can be summarized as follows:

(1) Dendrimers in the L_1-based series exhibit lamellar mesophases. The DAB compounds (DAB$[L_1]_{8-64}$, Figure 2) show two enantiotropic mesophases, a low-temperature SmC phase and a SmA phase. The mesomorphic temperature range is largely the same for n = 16, 32, and 64. A nematic mesophase is also observed for the first generation (n = 4). Let us remember that the PAMAM homologous dendrimers (series PAMAM$[L_1]_n$, Figure 3) only show a SmA mesophase, regardless of the generation number.

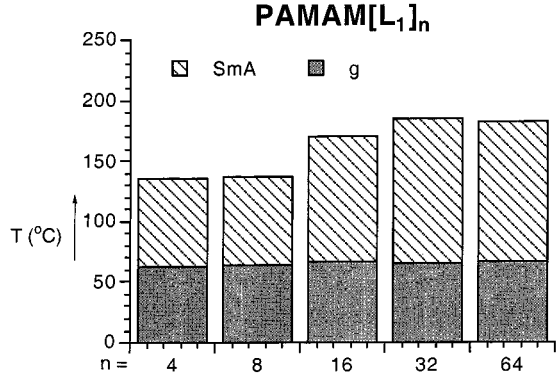

Figure 3. Phase behavior of PAMAM$[L_1]_n$.

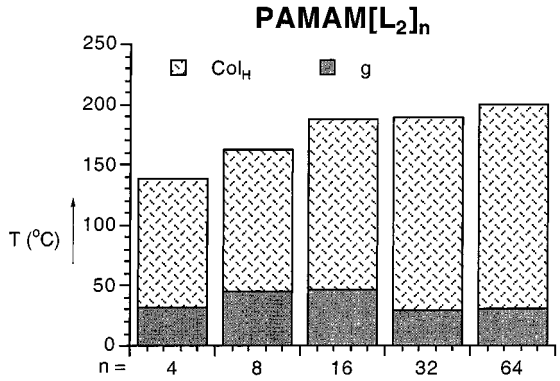

Figure 4. Phase behavior of PAMAM$[L_2]_n$.

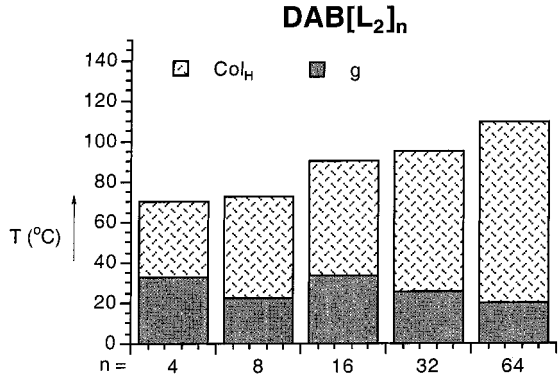

Figure 5. Phase behavior of DAB$[L_2]_n$.

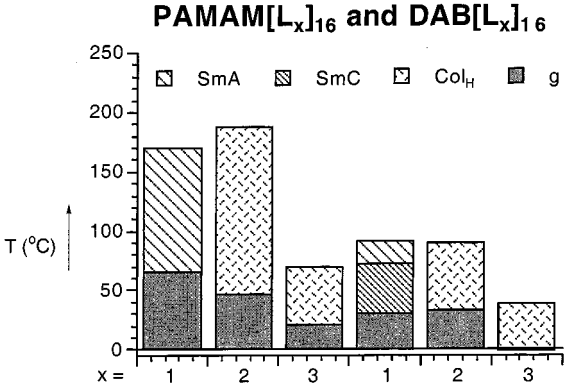

Figure 6. Phase behavior of PAMAM$[L_x]_{16}$ and DAB$[L_x]_{16}$.

(2) The series PAMAM$[L_2]_n$ (Figure 4) and DAB$[L_2]_n$ (Figure 5), as well as the two dendrimers PAMAM$[L_3]_{16}$ and DAB$[L_3]_{16}$ (Figure 6), display a single columnar phase, with broader temperature ranges for the PAMAM than for the DAB compounds.

Table 1. Layer Periodicity (d_{001}), Molecular Volume (V_M), Density (d), Molecular Area (A_M), Area per Mesogenic Unit (a_u), Thicknesses of the Different Molecular Parts Constituting the Lamellae (d_{Ar}, d_{Br}, and d_{Ch}), and Tilt Angles Experimentally Found for the PAMAM[L_1]$_n$ Compounds in the Smectic Phase

compound	T (°C)	mesophase	d_{001} (Å)	V_M (Å^3)	d (g cm^{-3})	A_{Mol} (Å^2)	a_u (Å^2)	d_{Ar} (Å)	φ (°)	d_{Br} (Å)	d_{Ch} (Å)
PAMAM[L_1]$_4$	22	SmA	51.9	3195	1.059	61.5	30.7	9.1_5	45.3	14.2	9.7
	100	SmA	46.0	3390	0.998	73.7	36.8	8.1	51.4	12.5	8.6_5
PAMAM[L_1]$_8$	22	SmA	57.2	7150	1.039	125	31.2	9.1	45.6	20.0	9.5
	120	SmA	43.0	7700	0.965	179	44.8	6.7_5	58.7	15.0	7.2_5
PAMAM[L_1]$_{16}$	22	SmA	59.3	15 070	1.029	254	31.7	8.9	39.5	22.7	9.4
	120	SmA	47.0	16 230	0.956	345.3	43.2	7.0	57.4	18.0	7.5
PAMAM[L_1]$_{32}$	22	SmA	60.5	30 900	1.025	510.7	31.9	8.9	39.8	24.1	9.3
	150	SmA	43.0	33 950	0.933	789.6	49.3	6.15	61.7	17.1	6.8
PAMAM[L_1]$_{64}$	22	SmA	61.1	62 560	1.023	1023.9	32	8.8_5	39.9	24.8	9.3
	150	SmA	48.0	68 740	0.931	1432	44.7	6.8	58.5	19.4	7.5

Table 2. Layer Periodicty (d_{001}), Molecular Volume (V_M), Density (d), Molecular Area (A_M), Area per Mesogenic Unit (a_u), Thicknesses of the Different Molecular Parts Constituting the Lamellae (d_{Ar}, d_{Br}, and d_{Ch}), and Tilt Angles Experimentally Found for the DAB[L_1]$_n$ Compounds in the Smectic Phase

compound	T (°C)	mesophase	d_{001} (Å)	V_M (Å^3)	d (g cm^{-3})	A_{Mol} (Å^2)	a_u (Å^2)	d_{Ar} (Å)	φ (°)	d_{Br} (Å)	d_{Ch} (Å)
DAB[L_1]$_8$	70	SmC	52.0	6120	1.035	117.7	29.4	10.0	39.7	10.9	10.5_5
	95	SmA	53.0	6230	1.017	117.5	29.4	10.1	39.0	11.1	10.8
DAB[L_1]$_{16}$	22	g SmC	52.0	12 040	1.072	231.5	28.9	9.8	41.1	11.9	10.25
	70	SmC	51.0	12 520	1.031	245.5	30.7	9.6	42.5	11.6	10.1
	90	SmA	46.5	12 710	1.015	273.3	34.1	8.7	48.0	10.6	9.2_5
DAB[L_1]$_{32}$	22	g SmC	53.5	24 350	1.070	455.1	28.4	9.9	40.4	12.7	10.5
	65	SmC	51.8	25 220	1.033	486.9	30.4	9.6	42.4	12.3	10.1_5
	90	SmA	46.5	25 700	1.013	552.7	34.5	8.6_5	48.3	11.0	9.1
DAB[L_1]$_{64}$	22	g SmC	55.0	48 975	1.068	890	27.8	10.1_5	38.7	13.3	10.7
	60	SmC	55.0	50 515	1.036	918	28.7	10.2	38.3	13.2	10.7
	95	SmA	48.0	51 870	1.010	1080.6	33.8	8.8_5	47.2	11.5	9.4

(3) Within both the PAMAM and DAB series with one or two chains per mesogenic unit, T_g does not vary significantly, and the temperature ranges of the mesophases for the higher generations (n = 16, 32, and 64) are comparable.

(4) The PAMAM[L_3]$_{16}$ and DAB[L_3]$_{16}$ dendrimers show a drastic decrease in T_i compared with third-generation L_2-based dendrimers. Therefore, an increase from two to three terminal chains in the mesogenic units contributes to a decrease of the stability domain of the columnar mesophase.

(5) Finally, the PAMAM derivatives exhibit more stable mesophases than the DAB derivatives (higher T_i values but similar T_g's). This could be due to the existence of intra- and intermolecular H bonds in the polyamidoamines (absent in the polypropyleneimines), which very likely contribute somewhat to making the central branching core rigid and enhancing the cohesion of the supramolecular lamellae or columns.

X-ray Diffraction Studies

Temperature-dependent X-ray diffraction experiments were systematically carried out to identify unequivocally the nature of the mesophases of all of the compounds reported here. The presentation of the data is split into two distinct parts: the first part corresponds to the L_1-based PAMAM and DAB dendrimers showing lamellar mesophases, and the second part corresponds to the L_2- and L_3-based homologous dendrimers that show only columnar mesophases. The XRD data and the specific calculated parameters relative to each family of mesophases are gathered in Tables 1−4.

Smectic Phases. The mesophase temperature ranges determined by XRD are in agreement with those measured by DSC, and all of the L_1-based systems prepared show mesomorphic behavior. The XRD patterns, recorded at several temperatures within the given mesomorphic range, are all qualitatively similar and contain a set of two, and in some cases three, equally spaced, sharp peaks in the small-angle region, with the intensity of the reflections decreasing with increasing Bragg angles. The reciprocal spacings are found in the ratio 1:2:3, characteristic of a lamellar morphology. A diffuse scattering halo in the wide-angle region is also observed, indicating the liquilike order within the smectic layers. These results are consistent with smectic mesophases, confirming the POM observations.

The lamellar periodicities of the PAMAM[L_1]$_n$ compounds measured at various temperatures are collected in Table 1. The temperature dependence of the smectic periodicity is systematically the same for all of the PAMAM compounds, in that it is almost invariant with increasing temperature up to 100 °C, and then it drops abruptly above this temperature. This is fairly common behavior in smectic liquid crystals, which is due to the increasing molecular disorder within the planes of the layers, consequently including a partial breakdown of the layers. Furthermore, the layer periodicity does not vary drastically despite the exponential increase of the molecular size, an indication that the molecular volume, on going from one generation to the next, likely expands within the plane of the layer.

As for the PAMAM series, the layer periodicity of the four DAB[L_1]$_x$ (x = 8, 16, 32, and 64) compounds varies almost independently of the generation number (Table 2), leading to the same conclusion as above in that the volume expansion of the molecules on increasing generation occurs in the planes of the layers. However, the dependence of the layer spacings on temperature is rather unusual. Indeed, in the case of the two-mesophase compounds (SmA and SmC phases), the periodicity of the tilted smectic phase was found to be larger than that measured for the SmA phase. A possible explanation for this phenomenon is to consider a SmA phase in which the aromatic segments of the dendritic molecules are randomly tilted with respect to the normal of the plane of the layer but with local fluctuations of the tilt angle (i.e., there is no long-range correlation of

the tilt angle or the tilt plane). This is a comparable thermal behavior comparable to that observed for the PAMAM series (d_{001} of the SmA is temperature-independent up to 100 °C and then drops), although, for the DABs, the drop in lamellar thickness occurs at the transition between two mesophases (at the SmC-to-SmA phase transformation) rather than within the same single mesophase only.

Thus, the PAMAM and DAB dendrimers show different thermal behaviors. First, a two-mesophase behavior (SmC and SmA) is observed for the DAB systems, whereas only a SmA phase is observed for the PAMAM systems. Second, the layer spacings of the DAB compounds are much smaller than those of the PAMAM compounds for equivalent generation numbers. In addition, the clearing temperatures are lower in the DAB systems than in the PAMAM systems, whereas the melting temperatures are in the same range, consequently leading to narrower mesomorphic temperature ranges. This emphasizes the lower thermodynamic stability of the former systems. The differences between these two series seem to be connected to the volume of the preexisting dendritic core (this is indeed the unique structural variation) and to the absence of H bonds within the DAB dendritic scaffold. The length of the spacer between two branching points in the DAB system is much smaller than in the PAMAM case, and therefore, for the same generation number, the core volume of the DAB is smaller than that of the PAMAM. This also leads, for the same number of branches, to a more limited thermal expansion behavior.

Molecular Organization within the Smectic Mesophases. For all of these compounds, the mesogenic units are necessarily arranged in a pseudoparallel fashion to allow for the formation of lamellar mesophases. The molecular conformation of the dendritic molecule must adopt an anisotropic shape such as the shape of a cylindrical object. Therefore, the molecules must be elongated along the cylinder axis. For this to be the case, the mesogenic units likely extend up and down from the molecular center, namely, the dendritic part (Figure 1). This parallel arrangement further reveals the amphipathic character of the molecule (a diblock rod molecule), which contributes to some degree to the mesophase stability. To test whether this molecular conformation is realistic, the molecular areas for all of these molecules at different temperatures, as well as the areas per mesogenic unit, were calculated (Tables 1 and 2). The molecular area, A_{Mol}, is directly obtained from the molecular volume, V_M, and the layer periodicity, d (d_{001}), according to $A_{Mol} = V_M/d$. It is also related to the area per mesogenic unit, a_u, considering that, statistically, one-half of the mesogenic units extend on one side and the other half on the other side of the dendritic core, i.e., A_{Mol} is proportional to one-half of the number of mesogenic units ($x = 1$ and $n = 8, 16, 32, 64$)

$$a_u = \frac{A_{Mol}}{\frac{xn}{2}} = 2\frac{A_{Mol}}{n}$$

The calculated global molecular areas and areas per mesogenic unit are indeed in relatively good agreement with such a parallel arrangement. The molecular area increases linearly with n in all cases, evidence that the expansion of the molecules occurs in the plane of the layer with increasing generation number (Figure 7). For

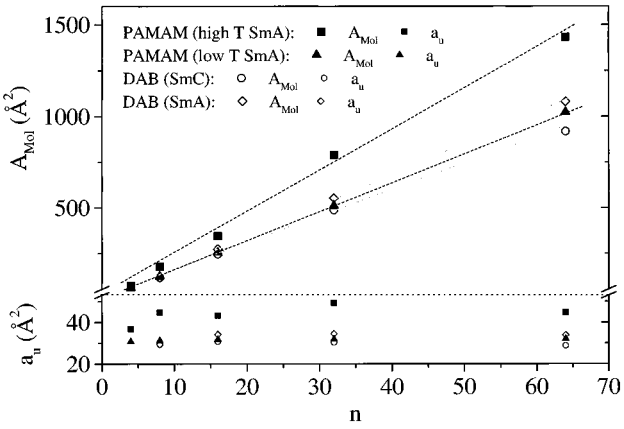

Figure 7. Molecular areas and areas per mesogenic unit as functions of T and n.

DAB systems, the area per mesogenic unit found for the SmC phase ($a_u = 30$ Å^2) is consistent with the molecular area found for the model compound in its SmC phase (K • 66 • SmC • 70.5 • N • 78 • I), $a_L = 24$ Å^2. However, the area found for the molecules in the upper mesophase ($a_u = 33$ Å^2) deviates quite substantially from what is usually expected for SmA phases. For the PAMAM series, which shows only a SmA phase, the area per mesogenic group is even higher than that for the DAB series ($a_u = 31$ Å^2 in the low-temperature range and 44 Å^2 at higher temperature). The areas per mesogenic unit in the SmC phase are large because the mesogenic units are tilted with respect to the layer normal. However, the high value found in the SmA phase, which is much larger than expected in such a phase (usually around 22−25 Å^2), is rather striking because it would correspond to a larger molecular tilt (Tables 1 and 2), which is unusual in such mesophase, or to some interdigitation of terminal chains. Judging from the POM observations, the texture of this mesophase showed large homeotropic regions, which led to the assumption that the mesophase is uniaxial. To agree with such an assumption (and with the optical observations), one has to consider layers where the rigid units are tilted with respect to the layer normal but where no correlation of the tilt angle and tilt plane exists. In other words, the relative disordered distribution of the rigid parts yields an apparent zero tilt angle and then a uniaxial mesophase.

The molecular tilt angles can be calculated if the volume occupied by the aromatic segments of one molecule, V_{Ar};[13] the thickness of the aromatic sublayer, d_{Ar}; and the length of the aromatic core, L_0 ($L_0 = 13$ Å), are known. As in block copolymers, the volume fraction of the aromatic slab, X_{Ar}, is deduced from the ratio $X_{Ar} = V_{Ar}/V_M$. Then, d_{Ar}, the thickness of one aromatic slab, is given by

$$d_{Ar} = {}^1/_2 X_{Ar} d$$

and φ, the tilt angle, is defined by its cosine

$$\cos\varphi = \frac{d_{Ar}}{L_0} = {}^1/_2 X_{Ar}\frac{d}{L_0}$$

In the SmC phase, the molecular tilt angle is found to be between 38 and 48°, whereas in the SmA phase, the tilt angle varies between 39 and 50° for the DAB systems and between 40 and 58° for the PAMAM systems.

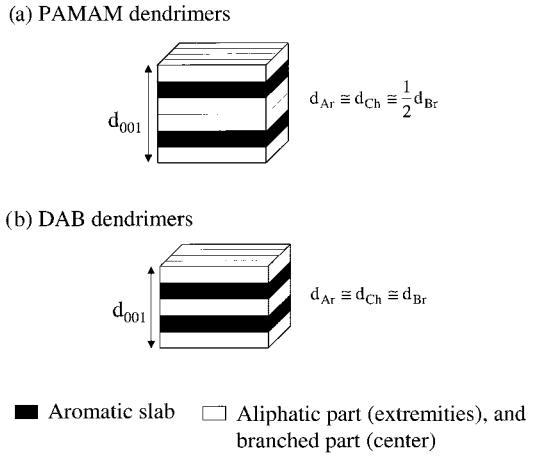

Figure 8. Illustration of the two different smectic morphologies generated by the (a) PAMAM and (b) DAB dendrimers.

On the basis of these calculations, the following explanations are able to account for the decrease in the layer spacings on going from a SmC to a SmA mesophase and, consequently, for the increase in the area per mesogenic unit. In the SmA phase, the mesogenic groups are tilted with respect to the layer because of large local orientational fluctuations. They are not tilted along a preferential direction as in the SmC phase but, rather, are distributed in space along a mean direction, a director, leading to an uniaxial type of mesophase. These fluctuations in the orientational order are a consequence, on one hand, of the restricted length of the dendritic branches in the DAB systems rendering the parallel arrangement of the mesogenic units difficult and, on the other hand, of the limit of expansion in the direction normal to the layer of the DAB flexible core (because of thermal expansion, the latter has to occupy a greater volume). In other words, the conformation of the branched dendrimer is distorted from a pseudocylindrical to a flattened and squeezed spheroidal conformation, while the mesogenic groups are forced to tilt to satisfy this dilation and to be arranged along one direction (SmC phase) or without preferential orientation (SmA phase). Similar explanations can be given for the SmA phase of the PAMAM systems.

To gain more insight into the lamellar supramolecular organization based on microphase separation between the different molecular regions, the thicknesses of the different sublayers were also calculated. Knowledge of the thicknesses of the dendritic and aliphatic sublayers, d_{Br} and d_{Ch}, respectively, can bring about some important information, especially as far as the degree of microsegregation is concerned. Thus, d_{Br} and d_{Ch} were calculated in the same manner as d_{Ar}.[14]

These calculations based on molecular areas are valid in both chain-interdigitation and chain-folding cases (which lead to the same model). Note that chain−aromatic and aromatic−aromatic interdigitation models have been excluded for unsatisfactory filling requirements conditions and for large divergence with experimental data. Two modes of temperature-independent lamellar supramolecular organizations have been extrapolated: (i) The first mode is exclusively associated with the PAMAM compounds in the SmA phase (Figure 8a), where the equality $\langle d_{Ar} \rangle \approx \langle d_{Ch} \rangle \approx \langle d_{Br} \rangle/2$ is verified. For example, $\langle d_{Ar} \rangle \approx 9.0$ Å, $\langle d_{Ch} \rangle \approx 9.5$ Å, and $\langle d_{Br} \rangle \approx 21.1$ Å at 22 °C for PAMAM$[L_1]_n$. (ii) The second mode is exclusively observed for the DAB$[L_1]_n$ compounds (Figure 8b) where the equality $\langle d_{Ar} \rangle \approx \langle d_{Ch} \rangle \approx \langle d_{Br} \rangle$ is almost satisfied. For example, $\langle d_{Ar} \rangle \approx 9.9$ Å, $\langle d_{Ch} \rangle \approx 10.5$ Å, and $\langle d_{Br} \rangle \approx 12.0$ Å at 60−70 °C for DAB$[L(10)_1]_n$ ($n = 8-64$).

Although these results do not completely explain why, in some cases, a SmA phase is seen whereas, in other cases, SmC and SmA phases are obtained, one can nevertheless notice some interesting aspects. First, recall that the monomer itself shows mainly a nematic phase, which completely disappears once a collection of such monomers is attached to a dendritic scaffold. Because the branched and aromatic parts are chemically linked, the smectic phase represents the most stable thermodynamic state of organization as for block copolymers in a lamellar morphology (mode 1 is more efficient than mode 2). Mesomorphism in this case has been strongly improved through the layering of the system. This confirms, once again, the strong analogy between liquid-crystal dendrimers and segmented AB block copolymers; here, microphase separation occurs immediately at the molecular level, i.e., at the dendrimer level. Moreover, the differences observed between the PAMAM and DAB systems are clearly related to how the aromatic interface is affected by the dendritic scaffold. The volume expansion of the dendrimer drastically influences the organization of the aromatic segments. It seems that, because of the nature of the preexisting dendrimer (structure and possibility for H bonds) and the temperature change, the internal dendritic core will adopt either a more pronounced prolate shape (or disklike) or a more oblate shape (ellipsoid), thus influencing the distribution in space of the rigid parts.

In summary, the general molecular organizations within the smectic phases are similar for the two series of compounds and can be described as follows: The conformationally disordered dendritic network occupies the central part of the smectic layers, with a thickness d_{Br}, sandwiched between two aromatic sublayers (d_{Ar}), in which the mesogenic groups are more or less aligned along a preferred direction, with a correlation of the tilt angle for the SmC phase and no correlation for the SmA phase. The aromatic slabs are coated by layers of disordered and molten aliphatic chains (d_{Ch}). Such a model is in agreement with the physical measurements (lamellar periodicities and molecular volumes), and the analogy with the lamellar morphology observed in block copolymers is once again reinforced.

Columnar Mesophases. Qualitatively similar X-ray patterns were obtained for all of the two- and three-chain systems studied here, regardless of the number of peripheral aliphatic chains (two or three) or the nature of the dendritic matrix (PAMAM or DAB). The X-ray patterns consist of a diffuse scattering halo in the wide-angle region, corresponding to the liquidlike disorder, and two, and sometimes three, sharp reflections in the small-angle region, corresponding to the reciprocal spacings in the ratios of 1, $\sqrt{3}$, and $\sqrt{4}$, with the corresponding indexes (hk) = (10), (11), and (20), indicating two-dimensional hexagonal packing of columns. Some trends can be immediately observed. The structural variations (number of aliphatic chains, type of dendritic scaffold) have no influence on the nature of the mesophase: all of the compounds show a Col_H mesophase, and the measured spacings d_{10} per family of compounds have almost identical values with increasing generation number.

Table 3. Molecular Characteristics and Structural Parameters[a] of the Col_H Phases as Functions of Generation Number, Temperature, and Number of Chains for the DAB[$L_{2,3}$]$_n$ Compounds

compound	T (°C)	mesophase	d_{10} (Å)	V_M (Å^3)	d (g cm^{-3})	s (Å^2)	X	N_{Ch}	N_{Mol}
DAB[L_2]$_4$	60	Col_H	49.8	4020	1.017	2864	0.39	24.7	3.1
	70	Col_H	50.0	4055	1.009	2887	0.39	24.7	3.1
DAB[L_2]$_8$	60	Col_H	50.5	8320	1.011	2945	0.41	25.7	1.6
	70	Col_H	48.6	8390	1.003	2727	0.41	24.6	1.5_5
DAB[L_2]$_{16}$	60	Col_H	55.9	16920	1.008	3608	0.42	28.7	0.9
	70	Col_H	54.8	17060	0.999	3468	0.42	28.0	0.9
DAB[L_2]$_{32}$	70	Col_H	52.2	34395	0.999	3146	0.42	26.9	0.4
	80	Col_H	51.6	34680	0.990	3075	0.42	26.5	0.4
	90	Col_H	51.15	34960	0.983	3021	0.43	26.3	0.4
DAB[L_2]$_{64}$	90	Col_H	50.4	70205	0.982	2933	0.42	25.8	0.2
	100	Col_H	49.85	70770	0.974	2869	0.42	25.4	0.2
DAB[L_3]$_{16}$	22	Col_H	41.75	20930	1.023	2013	0.32	19.0	0.4

[a] First-order reflection (d_{10}), columnar cross section (s), molecular volume (V_M), density (d), volume fraction (X), number of chains (N_{Ch}), and number of molecules (N_{Mol}) per columnar slice of thickness $\langle h \rangle$ (ca. 4.6 Å).

Table 4. Molecular Characteristics and Structural Parameters[a] of the Col_H Phases as a Function of Generation Number, Temperature, and Number of Chains for the PAMAM[$L_{2,3}$]$_n$ Compounds

compound	T (°C)	mesophase	d_{10} (Å)	V_M (Å^3)	d (g cm^{-3})	s (Å^2)	X	N_{Ch}	N_{Mol}
PAMAM[L_2]$_4$	100	Col_H	46.8	4565	0.967	2527	0.44	24.0	3.0
PAMAM[L_2]$_8$	100	Col_H	52.5	9935	0.956	3178	0.49	28.7	1.8
PAMAM[L_2]$_{16}$	100	Col_H	51.5	20 680	0.951	3065	0.51	28.8	0.9
PAMAM[L_2]$_{32}$	100	Col_H	58.2	42 170	0.948	3912	0.52	32.8	0.5
PAMAM[L_2]$_{64}$	100	Col_H	54.9	85 150	0.947	3483	0.52	31	0.2_5
PAMAM[L_3]$_{16}$	25	Col_H	56.4	24 015	1.000	3673	0.40	28.8	0.6
	40	Col_H	55.4	24 320	0.988	3544	0.40	28.2	0.6
	60	Col_H	52.2	24 730	0.971	3146	0.40	26.3	0.5_5

[a] First-order reflection (d_{10}), columnar cross section (s), molecular volume (V_M), density (d), volume fraction (X), number of chains (N_{Ch}), and number of molecules (N_{Mol}) per columnar slice of thickness $\langle h \rangle$ (ca. 4.6 Å).

In the DAB[L_2]$_n$ compounds, d_{10} varies between 49 and 55 Å with generation number. However, rather large variations of the d_{10} periodicity are observed when compared to the PAMAM homologous compounds: d_{10} is smaller in the DAB compounds than in the PAMAM compounds for the same generation number (Tables 3 and 4). The size of the hexagonal cells changes when an extra chain is grafted onto the terminal promesogenic unit: on going from DAB[L_2]$_{16}$ to DAB[L_3]$_{16}$, d_{10} decreases, whereas it increases from PAMAM[L_2]$_{16}$ to PAMAM[L_3]$_{16}$.

Except for DAB[L_3]$_{16}$, the areas of the hexagonal lattice are very comparable for the two series of compounds. This might be an indication that the expansion of the dendritic core (the unique structural variation) occurs in only one direction, that is, along the columnar axis. As in the lamellar systems described above, the differences in the mesomorphic temperature range, and thus in the thermal stability, are likely because of the reduced volume of the DAB dendritic network compared to that of the PAMAMs and its limited thermal expansion.

Molecular Organization within the Columnar Mesophase. To understand the molecular arrangement of the different generations of dendrimers within the columnar mesophase, the same geometrical approach as used previously for the PAMAM[L_2]$_n$ series of dendrimers[6c] was applied. Our methodology consisted of determining the average number of aliphatic chains radiating from the rigid interface of the inner hard columnar core of thickness $\langle h \rangle$ and thus the corresponding number of molecules within this slice. It is important to point out that, in such systems, $\langle h \rangle$ does not have a particularly significant meaning, because the dendritic cores constituting the inner part of the columns are in a liquilike order conformation, so that one cannot consider a strict packing of disklike molecular assemblies in a perfect manner such as in a pile of plates. However, knowledge of this value allows for the calculation of a linear density along the columnar axis and a comparison with classical disklike systems. We have recently proposed a method for the analytical determination of $\langle h \rangle$ as a function of temperature.[6c,15] As above, the same definition and the same method for determining the specific molecular volume (V_M[13]) and the partial volumes (V_{Br},[13] V_{Ch},[13] and V_{Ar}[16]) were used. The cross-sectional area of the column, s, was deduced experimentally from XRD measurements. All of these structural parameters are represented in Figure 9.

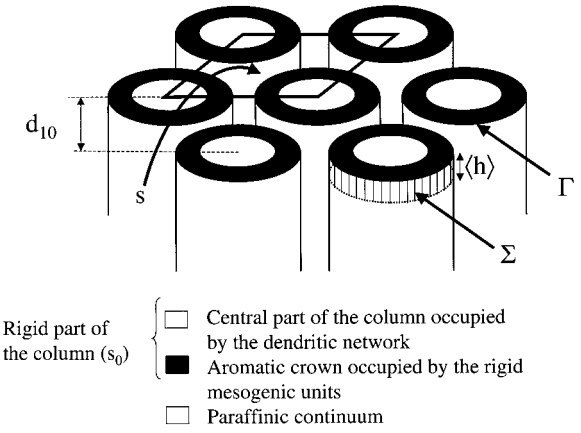

Figure 9. Location of the different partial volumes associated with the different segments of the dendrimers when assembled into columns packed into a hexagonal bidimensional lattice.

The volume fraction of the central core of the column, X (equal to the volume fraction of the dendritic and aromatic constitutive parts of the molecule) is expressed by $X = (V_{Br} + V_{Ar})/V_M$. It is now possible to calculate s_0, which corresponds to a fraction of s (equal to the area of the elementary cell of the hexagonal phase), using

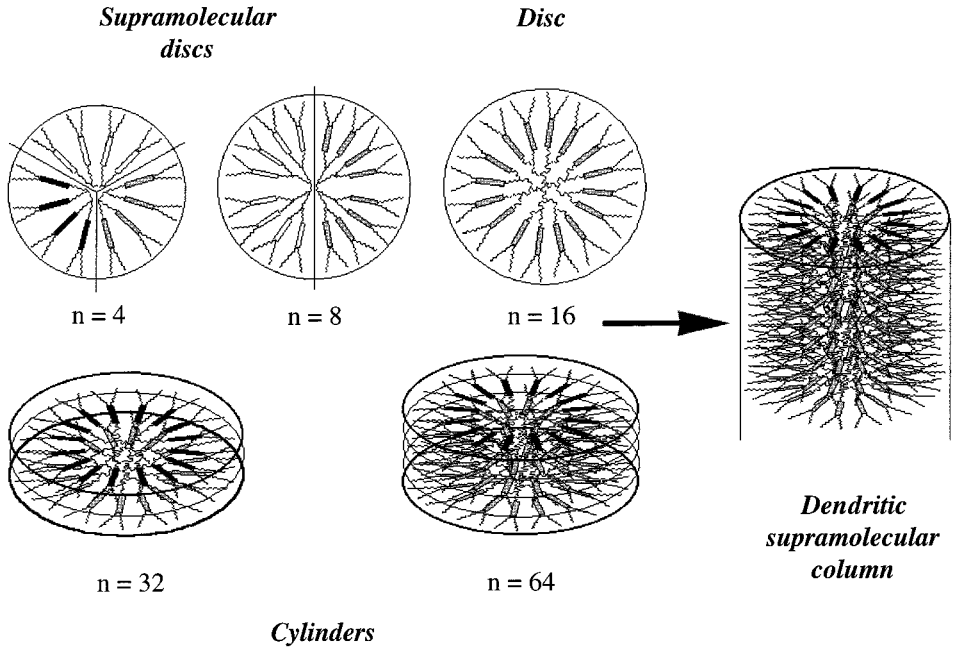

Figure 10. Schematic representation of the self-assembly process of the different generation dendrimers with $x = 2$ into columns.

$s_0 = sX = (2/\sqrt{3})Xd_{10}^2$. The corresponding perimeter of s_0, Γ, and the associated radial area of a slice of thickness $\langle h \rangle$, Σ, which are circular and cylindrical, respectively, because of the symmetry of the Col_H mesophase, are given by

$$\Gamma = 2\sqrt{\pi X s} \quad \text{and} \quad \Sigma = \Gamma\langle h \rangle = 2g\sqrt{\pi X s \sigma}$$

The number of chains radiating from this interface Σ, N_{Ch}, as well as the number of molecules, N_{Mol}, that can be accommodated within such a columnar slice can be calculated according to the following equations

$$N_{Ch} = \frac{\Sigma}{\sigma} = 2g\sqrt{\frac{\pi X s}{\sigma}} \quad \text{and} \quad N_{Mol} = \frac{N_{Ch}}{N}$$

where N is the number of chains per molecule. ($N = 2n$ for DAB$[L_2]_n$ and PAMAM$[L_2]_n$, and $N = 48$ for DAB$[L_3]_{16}$ and PAMAM$[L_3]_{16}$.)

The results (Tables 3 and 4) show very good agreement with those previously obtained in the related PAMAM systems. On average, the columns are formed by the self-assembly of the dendritic molecules into supramolecular disklike aggregates (Figure 10). These disks of thickness $\langle h \rangle$ are filled with an average number of molecules that depends on the generation number according to a geometrical law. It was previously found that, statistically, more than three PAMAM$[L_2]_4$ molecules are needed to fill one columnar slice, whereas about two PAMAM$[L_2]_8$ and only one PAMAM$[L_2]_{16}$ are necessary to satisfy the volume requirements. For the last two generations, the molecular size is so large that more than one slice is needed to accommodate one molecule in the available volume. Thus, two and four "disks" are necessary for PAMAM$[L_2]_{32}$ and PAMAM-$[L_2]_{64}$ molecules, respectively.[6c] It was also clearly stated that, because the system is not static, diffusion of one molecule or one part of it from one slice to another certainly occurs, thus giving rise to many other intermediate possibilities. In the DAB$[L_2]_n$ series, exactly the same tendency is observed. For reasons similar to those mentioned in the lamellar case, such as the molecular conformation of the dendritic core and the geometric constraints resulting from the volume of the inner core, the mesogenic units are not arranged in a purely radiative disposition. Indeed, because of the restricted size of the preexisting DAB dendrimers compared to the PAMAMs, the volume expansion of the dendrimers occurs out-of-plane sooner (from the second generation, $n = 8$, onward), i.e., in a direction parallel to the columnar axis,[6c] and as a consequence, the mesogenic units are tilted with respect to both the hexagonal lattice plane and the columnar axis. This has been verified by the calculation of the inner interface separating the mesogenic units from the branching dendrimeric part. This calculation was carried out in a manner identical to that explained above, but considering the volume fraction of the dendritic part only, X^* ($X^* = V_{Br}/V_M$). It showed that, to compensate for the area of the inner interface, the mesogenic units are tilted equally within the plane of the hexagonal cell and out of this plane and the thickness of the slice, $\langle h \rangle$, is consequently larger. In other words, the conformation of the branched dendrimer is distorted from a pseudocylindrical (prolate) to an elongated ellipsoidal (oblate) conformation. Thus, in the DAB$[L_2]_n$ series, 3.1, 1.6, 0.9, 0.4, and 0.2 molecules or fractions of molecules (for $n =$ 4, 8, 16, 32, and 64, respectively) are needed to fill one columnar slice, which is slightly less than the amounts required for the PAMAM system for the same slice thickness $\langle h \rangle$, the difference nevertheless being negligible. For PAMAM$[L_3]_{16}$ and DAB$[L_3]_{16}$, respectively, slightly less than $^2/_3$ and ca. $^1/_2$ of a molecule are needed to satisfy these filling requirements. Because of the larger number of terminal chains per dendrimer (48 chains), it is expected that a smaller number of molecules is required in a slice than for the analogous L_2-based systems (32 chains). Here also, the same discrepancy between the DAB and PAMAM dendrimers is observed; however, the difference in number of molecules is not as negligible as above. This is related to the volume of DAB being smaller than that of PAMAM and to the geometric constraints being stronger. The

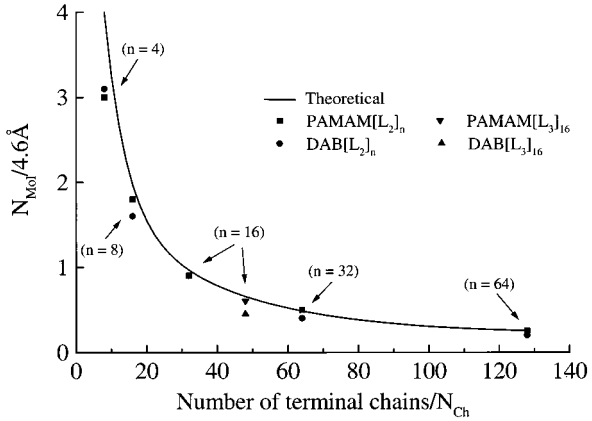

Figure 11. Number of molecules per columnar slice of thickness $\langle h \rangle$ (ca 4.6 Å) versus number of terminal alkoxy chains (thus generation number) compared to the theoretical variation (line in bold).

consequence is a smaller available volume for space filling. Thus, on one hand, only one-half of a molecule can be fitted in, and on the other hand, the expansion of this volume is more pronounced along the columnar axis than in the transverse direction.

On the graph in Figure 11 is represented the number of molecules per columnar slice $\langle h \rangle$ (nearly equal to 4.6 Å) as a function of the number of terminal chains per dendrimer, which is compared to a simple theoretical variation (4, 2, 1, 0.5, and 0.25 molecules per slice with increasing generation number). The theoretical curve, which follows a geometrical law, was obtained by assuming that, from every slice of thickness $\langle h \rangle$, 32 chains radiate, which corresponds to one L_2-based dendrimer of the third generation. One can see that shifts from the theoretical estimation are very small and thus fairly good agreement is obtained between the calculated variation and the experimental determinations.

It is important to note that these shifts from the theoretical law occur in the first part of the graph only, that is, in the case of the self-assembly into supramolecular disks prior to the stacking into columns. In this case, the molecules benefit from more degrees of freedom and, therefore, are not as constrained as in the higher-generation molecules to occupy the available volume. They can thus adopt several conformations, expand in the plane of the supramolecular disk, and exchange positions with their neighbors, i.e., in the transverse direction (intra- and intercolumnar diffusion) or along the columnar axis (intracolumnar diffusion only).

To summarize, the series of compounds displaying the columnar phase all behave in the same manner. They show the same type of mesophase (Col_H) with relatively close cell dimensions, regardless of the dendritic cores (PAMAM or DAB) or the number ($x = 2$ or 3) of terminal alkoxy chains. The only difference between the DAB and PAMAM series is related to the higher thermal stability of the PAMAM systems, a consequence of additional inter- and intramolecular H-bonding interactions. The columns result from the aggregation of the molecules into supramolecular disks (for the first and second generations), disks (for the third generation), or small cylinders (for the last two generations), which further self-organize into cylindrical columns. Such an aggregation process is favored by the fact that the molecules can adopt several conformations, depending on the number of generations and the number of terminal chains. These columns self-assemble into a 2-D hexagonal array to form a columnar hexagonal phase. At the same time, the disordered chains ensure the gliding of the columns with respect to each other and, thus, the fluidity and liquid-crystalline nature of the mesophase. Let us also recall that none of the two- and three-chain monomers were mesomorphic prior to attachment to the preexisting dendrimer scaffolds. Mesomorphism has thus been induced here as a result of the perfect disposition in space of the "monomer" according to a subtle microphase separation process.

Conclusions

In conclusion, we have shown in this paper that we have been able to generate mesomorphic properties in dendrimers of high molecular weight. This has been achieved through a simple chemical design, combined with the role of different types of intermolecular interactions. In the PAMAM series, hydrogen bonds between the amido groups contribute to the rigidity of the internal core, making it more rigid than the core in the DAB system, which lacks such H bonds. As a consequence, the mesomorphic properties are, on average, improved in the PAMAM compounds: wide mesophase temperature range, high clearing temperature. The interactions between the polarizable promesogenic units combined with the microphase segregation contribute to the stabilization of the aromatic sublayers (in the smectic phases) and the columnar cores (in the Col_H phase). The presence of one chain per mesogenic unit favors their parallel arrangement; hence, the lamellar morphology is promoted. It has been also shown that the mesomorphic behaviors observed in the two families of dendrimers, DAB and PAMAM, differ quite substantially from each other. The effect of the preexisting dendritic structure on the shape of the aromatic interface (oblate and prolate) has been highlighted. The increase in aliphatic chain density imposes a curved interface with the promesogenic units, the latter being forced to be radially arranged, hence inducing the columnar mesomorphism. We showed that the methodology used for the calculations of the molecular area in the lamellar systems and the interfacial area in the columnar systems allows for models to be proposed that satisfactorily describe the supramolecular organization within these mesophases. This geometrical approach can be generalized and used to study and understand the molecular arrangement in other mesomorphic systems produced by this type of end-functionalized liquid-crystalline dendrimers. Such predictions would lead to a better design of such macromolecules with precisely tuned mesomorphic properties.

Acknowledgment. This work was supported by the Comisión Interministerial de Ciencia y Tecnologia (Spain) (Projects MAT99-1009-CO2-02 and MAT2000-1293-CO2-01), the European Union (FMRX-CT97-0121 and HPRN-CT-2000-00016), and the French−Spanish cooperation program (Picasso HF1998-0144). B.D. thanks Dr. Antoine Skoulios and Dr Benoît Heinrich for instructive and helpful discussions and Prof. Yves Galerne for sharing his knowledge about textural defects in liquid crystals, which proved useful in some identifications.

Supporting Information Available: The techniques of characterization; the synthetic procedure; ^{1}H and ^{13}C NMR and IR listings; elemental analysis; and a table of thermodynamic data for the phase transitions of the new compounds. A typical X-ray pattern of a columnar phase. This material is available free of charge via the Internet at http://pubs.acs.org.

References and Notes

(1) (a) Tomalia, D. A.; Naylor, A. M.; Goddard, W. A., III. *Angew. Chem., Int. Ed. Engl.* **1990**, *29*, 138−175. (b) Issberner, J.; Moors, R.; Vögtle, F. *Angew. Chem., Int. Ed. Engl.* **1994**, *33*, 2413−2420. (c) Ardouin, N.; Astruc, D. *Bull. Soc. Chim. Fr.* **1995**, *132*, 875−909. (d) Newkome, G. R.; Moorefield, C. N.; Vögtle, F. In *Dendritic Molecules: Concepts, Synthesis and Perspectives*; VCH: Weinheim, Germany, 1996. (e) Ashton, P. R.; Boyd, S. E.; Brown, C. L.; Nepogodiev, S. A.; Meijer, E. W.; Peerlings, H. W. I.; Stoddart, J. F. *Chem. Eur. J.* **1997**, *3*, 974−984. (f) Zeng, F.; Zimmerman, S. C. *Chem. Rev.* **1997**, *97*, 1681−1712. (g) Matthews, O. A.; Shipway, N.; Stoddart, J. F. *Prog. Polym. Sci.* **1998**, *23*, 1−56. (h) Chow, H. F.; Mong, T. K. K.; Nongrum, M. F.; Wan, C. W. *Tetrahedron* **1998**, *54*, 8543−8660. (i) Fischer, M.; Vögtle, F. *Angew. Chem., Int. Ed.* **1999**, *38*, 884−905. (j) Inoue, K. *Prog. Polym. Sci.* **2000**, *25*, 453−571.

(2) (a) Skoulios, A.; Guillon, D. *Mol. Cryst. Liq. Cryst.* **1988**, *165*, 317−332. (b) Tschierske, C. *J. Mater. Chem.* **1998**, *8*, 1485−1508.

(3) Hyperbranched polymers with mesogenic branching units: (a) Percec, V.; Kawasumi, M. *Macromolecules* **1992**, *25*, 3843−3850. (b) Bauer, S.; Fischer, H.; Ringsdorf, H. *Angew. Chem., Int. Ed. Engl.* **1993**, *32*, 1589−1592. (c) Percec, V.; Chu, P.; Kawasumi, M. *Macromolecules* **1994**, *27*, 4441−4453. (d) Hanh, S. W.; Yun, S. Y. K.; Jin, J. I.; Han, O. H. *Macromolecules* **1998**, *31*, 6417−6425. Only one example of hyperbranched polymer with mesogenic end-groups was found: (e) Sunder, A.; Quincy, M. F.; Mülhaupt, R.; Frey, H. *Angew. Chem., Int. Ed.* **1999**, *38*, 2928−2930.

(4) Polysiloxane LC dendrimers: Ponomarenko, S. A.; Rebrov, E. A.; Boiko, N. I.; Vasilenko, N. G.; Muzafarov, A. M.; Freidzon, Y. S.; Shibaev V. P. *Polym. Sci. Ser. A* **1994**, *36*, 896−901.

(5) Polycarbosilane LC dendrimers: (a) Ponomarenko, S. A.; Rebrov, E. A.; Bobronsky, Y.; Boiko, N. I.; Muzafarov, A. M.; Shibaev, V. P. *Liq. Cryst.* **1996**, *21*, 1−12. (b) Lorenz, K.; Hölter, D.; Mühlhaupt, R.; Frey, H. *Adv. Mater.* **1996**, *8*, 414−416. (c) Coen, M. C.; Lorenz, K.; Kressler, J.; Frey, H.; Mülhaupt, R. *Macromolecules* **1996**, *29*, 8069−8076. (d) Lorenz, K.; Frey, H.; Stühn, B.; Mülhaupt, R. *Macromolecules* **1997**, *30*, 6860−6868. (e) Stark, B.; Stühn, B.; Frey, H.; Lach, C.; Lorenz, K.; Frick, B. *Macromolecules* **1998**, *31*, 5415−5423. (f) Ponomarenko, S. A.; Rebrov, E. A.; Boiko, N. I.; Muzafarov, A. M.; Shibaev, V. P. *Polym. Sci. Ser. A.* **1998**, *40*, 763−774. (g) Ryumtsev, E. I.; Evlampieva, N. P.; Lezov, A. V.; Ponomarenko, S. A.; Boiko, N. I.; Shibaev, V. P. *Liq. Cryst.* **1998**, *25*, 475−476. (h) Trahasch, B.; Stühn, B.; Frey, H.; Lorenz, K. *Macromolecules* **1999**, *32*, 1962−1966. (i) Richardson, R. M.; Ponomarenko, S. A.; Boiko, N. I.; Shibaev, V. P. *Liq. Cryst.* **1999**, *26*, 101−108. (j) Terunuma, D.; Kato, T.; Nishio, R.; Aoki, Y.; Nohira, H.; Matsuoka, K.; Kuzuhara, H. *Bull. Chem. Soc. Jpn.* **1999**, *72*, 2129−2134. (k) Richardson, R. M.; Whitehouse, I. J.; Ponomarenko, S. A.; Boiko, N. I.; Shibaev, V. P. *Mol. Cryst. Liq. Cryst.* **1999**, *330*, 167−174. (l) Ponomarenko, S. A.; Boiko, N. I.; Rebrov, E.; Muzafarov, A.; Whitehouse, I.; Richardson, R. M.; Shibaev, V. P. *Mol. Cryst. Liq. Cryst.* **1999**, *332*, 43−50. (m) Ponomarenko, S. A.; Boiko, N. I.; Shibaev, V. P.; Richardson, R. M.; Whitehouse, I. J.; Rebrov, E. A.; Muzafarov, A. M. *Macromolecules* **2000**, *33*, 5549−5558. (n) Ponomarenko, S. A.; Boiko, N. I.; Shibaev, V. P.; Magonov, S. N. *Langmuir* **2000**, *16*, 5487−5493. (o) Boiko, N. I.; Zhu, X.; Vinokur, R.; Rebrov, E.; Muzafarov, A.; Shibaev, V. P. *Ferroelectrics* **2000**, *243*, 59−66.

(6) Polyamidoamine LC dendrimers: (a) Suzuki, K.; Haba, O.; Nagahata, R.; Yonetake, K.; Ueda, M. *High Perform. Polym.* **1998**, *10*, 231−240. (b) Barberá, J.; Marcos, M.; Serrano, J. L. *Chem. Eur. J.* **1999**, *5*, 1834−1840. (c) Marcos, M.; Giménez, R.; Serrano, J. L.; Donnio, B.; Heinrich, B.; Guillon, D. *Chem. Eur. J.* **2001**, *7*, 1006−1013.

(7) Polypropyleneimine LC dendrimers: (a) Stebani, U.; Lattermann, G. *Adv. Mater.* **1995**, *7*, 578−581. (b) Seitz, M.; Plesnivy, T.; Schimossek, K.; Edelmann, M.; Ringsdorf, H.; Fischer, H.; Uyama, H.; Kobayashi, S. *Macromolecules* **1996**, *29*, 6560−6574. (c) Cameron, J. H.; Facher, A.; Latterman, G.; Diele, S. *Adv. Mater.* **1997**, *9*, 398−403. (d) Baars, M. W. P. L.; Söntjens, S. H. M.; Fischer, H. M.; Peerlings, H. W. I.; Meijer, E. W. *Chem. Eur. J.* **1998**, *4*, 2456−2466. (e) Yonetake, K.; Suzuki, K.; Morishita, T.; Nagahata, R.; Ueda, M. *High Perform. Polym.* **1998**, *10*, 373−382. (f) Yonetake, K.; Masuko, T.; Morishita, T.; Suzuki, K.; Ueda, M.; Nagahata, R. *Macromolecules* **1999**, *32*, 6578−6586. (g) Barberá, J.; Marcos, M.; Omenat, A.; Serrano, J. L.; Martínez, J. I.; Alonso, P. J. *Liq. Cryst.* **2000**, *27*, 255−262.

(8) Other dendritic structures: (a) Stebani, U.; Lattermann, G.; Wittenberg, M.; Wendorf, J. H. *Angew. Chem., Int. Ed. Engl.* **1996**, *35*, 1858−1860. (b) Deschenaux, R.; Serrano, E.; Levelut, A. M. *Chem. Commun.* **1997**, 1577−1578. (c) Busson, P.; Ihre, H.; Hult, A. *J. Am. Chem. Soc.* **1998**, *120*, 9070−9071. (d) Busson, P.; Ôrtegren, J.; Ihre, H.; Gedde, U. W.; Hult, A. *Macromolecules* **2001**, *34*, 1221−1229.

(9) Closely related starlike LCs: (a) Kreuzer, F. H.; Mauerer, R.; Spes, P. *Makromol. Chem. Makromol. Symp.* **1991**, *30*, 215. (b) Sellinge, A.; Laine, R. M.; Chu, V.; Viney, C. *J. Polym. Sci. A: Polym. Chem.* **1994**, *32*, 3069. (c) Mehl, G. H.; Goodby, J. W. *Angew. Chem., Int. Ed. Engl.* **1996**, *35*, 2641−2643. (d) Mehl, G. H.; Goodby, J. W. *Mol. Cryst. Liq. Cryst.* **1997**, *303*, 15−21. (e) Mehl, G. H.; Saez, I. M.; Goodby, J. W. *Appl. Organomet. Chem.* **1999**, *13*, 261−272. (f) Mehl, G. H.; Thornton, A. J.; Goodby, J. W. *Mol. Cryst. Liq. Cryst.* **1999**, *332*, 455−461. (g) Chuard, T.; Deschenaux, R.; Hirsch, A.; Schönberger, H. *Chem. Commun.* **1999**, 2103−2104. (h) Saez, I. M.; Goodby, J. W. *Liq. Cryst.* **1999**, *26*, 1101−1105. (i) Elsäber, R.; Mehl, G. H.; Goodby, J. W.; Photinos, D. J. *Chem. Commun.* **2000**, 851−852.

(10) Supramolecular dendrimers: (a) Balagurusamy, V. S. K.; Ungar, G.; Percec, V.; Johansson, G. *J. Am. Chem. Soc.* **1997**, *119*, 1539−1555. (b) Hudson, S. D.; Jung, H. T.; Percec, V.; Cho, W. D.; Johansson, G.; Ungar, G.; Balagurusamy, U. S. K. *Science* **1997**, *278*, 449−452. (c) Percec, V.; Cho, W. D.; Mosier, P. E.; Ungar, G.; Yeardley, D. J. P. *J. Am. Chem. Soc.* **1998**, *120*, 11061−11070. (d) Hudson, S. D.; Jung, H. T.; Kewsuwan, P.; Percec, V.; Cho, W. D. *Liq. Cryst.* **1999**, *26*, 1493−1499. (e) Ungar, G.; Percec, V.; Holerca, M. N.; Johansson, G.; Heck, J. A. *Chem. Eur. J.* **2000**, *6*, 1258−1266. (f) Percec, V.; Cho, W. D.; Ungar, G.; Yeardley, D. J. P. *Angew. Chem., Int. Ed.* **2000**, *39*, 1597−1602. (g) Percec, V.; Cho, W. D.; Möller, M.; Prokhorova, S. A.; Ungar, G.; Yeardley, D. J. P. *J. Am. Chem. Soc.* **2000**, *122*, 4249−4250. (h) Percec, V.; Cho, W. D.; Ungar, G. *J. Am. Chem. Soc.* **2000**, *122*, 10273−10281. (i) Percec, V.; Cho, W. D.; Ungar, G.; Yeardley, D. J. P. *J. Am. Chem. Soc.* **2001**, *123*, 1302−1315.

(11) Willow-like dendrimers: (a) Percec, V.; Chu, P.; Ungar, G.; Zhou, J. *J. Am. Chem. Soc.* **1995**, *117*, 11441−11454. (b) Li, J. L.; Crandall, K. A.; Chu, P.; Percec, V.; Petschek, R. G.; Rosenblatt, C. *Macromolecules* **1996**, *29*, 7813−7819.

(12) Shape-persistent dendrimers: (a) Moore, J. S. *Acc. Chem. Res.* **1997**, *55*, 13377−13394. (b) Pesak, D. J.; Moore, J. S. *Angew. Chem., Int. Ed.* **1997**, *36*, 1636−1639. (c) Meier, H.; Lehmann, M. *Angew. Chem., Int. Ed.* **1998**, *37*, 643−645. (d) Meier, H.; Lehmann, M.; Kolb, U. *Chem. Eur. J.* **2000**, *6*, 2462−2469. (e) Lehmann, M.; Schartel, B.; Hennecke, M.; Meier, H. *Tetrahedron* **1999**, *55*, 13377−13394.

(13) The analysis is based on a simple additivity rule for the calculation of the specific volumes. V_M can be written as a sum of elementary volumes associated with the different segments of the dendritic molecule according to $V_M = V_{Br} + V_{Ar} + V_{Ch}$, where V_{Br}, V_{Ar}, and V_{Ch} are the volumes of the branched dendritic network, the aromatic rigid parts, and the aliphatic chains, respectively. The volume of one aromatic part with one aliphatic chain, $v_{Ar}^{(1)}$, was obtained experimentally by a dilatometry experiment carried out on a model compound having the structure of the terminal group, namely, *N*-decyl-4-decyloxybenzoyloxysalicylaldimine. The different volumes, V_{Br}, V_{Ar}, V_{Ch}, v_{CH_2}, and Δv_{CH_3} were calculated as follows (in Å^3 with T in °C): $V_{Ar} = nv_{Ar}^{(x)}$, $V_{Br} = (M_{Br}/M_{CH_2})v_{CH_2}$ and $V_{Ch} = 10nxv_{CH_2} + nx\Delta v_{CH_3}$. M_{Br} is the molecular weight of the dendritic part, and M_{CH_2} is the molecular weight of one methylene group (14.01 g mol^{-1}). The volume of one methylene group is given by $v_{CH_2} = 26.5616 + 0.020\,23T$, and $\Delta v_{CH_3} = 27.14 + 0.017\,13T + 0.000\,418\,1T^2$ represents the volume difference between a methyl and a methylene group. For the lamellar systems, $x = 1$, and $v_{Ar}^{(1)} = 276 + 0.31T - 0.000\,836\,2T^2$.

(14) $d_{Br} = X_{Br}d$ with $X_{Br} = V_{Br}/V_M$ and $d_{Ch} = {}^1/_2X_{Ch}d$ with $X_{Ch} = V_{Ch}/V_M$.

(15) $\langle h \rangle = g\sqrt{\sigma}$, where σ is the cross-sectional area of one methylene group, $V_{CH_2}/1.27$, and g is a geometric factor equal to 0.9763.

(16) V_{Ar} has different values than above because the terminal chains' substitution pattern is different. Thus, for the two-chain promesogenic group, $x = 2$, the volume of the elementary aromatic part is given by $v_{Ar}^{(2)} = 249.6 + 0.31T - 0.000\,836\,2T^2$ and for the three-chain system, $x = 3$, $v_{Ar}^{(3)} = 236.0 + 0.31T - 0.000\,836\,2T^2$.

MA010881+